

Cite this: *Chem. Sci.*, 2016, **7**, 6197

## A polymer acceptor with an optimal LUMO energy level for all-polymer solar cells†

Zicheng Ding,‡<sup>a</sup> Xiaojing Long,‡<sup>ab</sup> Chuandong Dou,\*<sup>a</sup> Jun Liu\*<sup>a</sup> and Lixiang Wang<sup>a</sup>

A key parameter for polymer electron acceptors is the lowest unoccupied molecular orbital (LUMO) energy level ( $E_{\text{LUMO}}$ ). For state-of-the-art polymer electron acceptors based on the naphthalene diimide (NDI) unit, their  $E_{\text{LUMO}}$  are low-lying and cannot be tuned, leading to a low open-circuit voltage ( $V_{\text{oc}}$ ) of the resulting all-polymer solar cells (all-PSCs). We report that polymer electron acceptors based on the double B $\leftarrow$ N bridged bipyridine (BNBP) unit exhibit tunable  $E_{\text{LUMO}}$  because of their delocalized LUMOs over polymer backbones. The  $E_{\text{LUMO}}$  of the copolymer of the BNBP unit and selenophene unit (P-BNBP-Se) is lower by 0.16 eV than that of the copolymer of the BNBP unit and thiophene unit (P-BNBP-T). As a result, the energy levels of P-BNBP-Se match well with the widely-used polymer donor, poly[(ethylhexyl-thiophenyl)-benzodithiophene-(ethylhexyl)-thienothiophene] (PTB7-Th). The electron mobility of P-BNBP-Se ( $\mu_{\text{e}} = 2.07 \times 10^{-4} \text{ cm}^2 \text{ V}^{-1} \text{ s}^{-1}$ ) is also higher than that of P-BNBP-T ( $\mu_{\text{e}} = 7.16 \times 10^{-5} \text{ cm}^2 \text{ V}^{-1} \text{ s}^{-1}$ ). While the all-PSC device based on the PTB7-Th:P-BNBP-T blend shows a moderate power conversion efficiency (PCE) of 2.27%, the corresponding device with P-BNBP-Se as the acceptor exhibits a PCE as high as 4.26%. Moreover, owing to the suitable  $E_{\text{LUMO}}$  of P-BNBP-Se, the all-PSC device of P-BNBP-Se shows a  $V_{\text{oc}}$  up to 1.03 V, which is higher by 0.22 V than that with the conventional NDI-based polymer acceptor. These results indicate that BNBP-based polymers can give all-PSCs with high PCEs, remarkably high  $V_{\text{oc}}$  values and small photon energy losses.

Received 22nd April 2016  
Accepted 14th June 2016

DOI: 10.1039/c6sc01756h

[www.rsc.org/chemicalscience](http://www.rsc.org/chemicalscience)

## Introduction

All-polymer solar cells (all-PSCs), which utilize polymers as both the electron donor and electron acceptor, have attracted much attention recently because of their great advantages over conventional polymer/fullerene PSCs.<sup>1</sup> These advantages include enhanced light absorption of polymer acceptors, low cost, and improved mechanical/thermal stability. Great progress in all-PSCs has been made by using absorption-complementary polymer donor/acceptors, optimizing the blend morphologies, or developing new polymer acceptors.<sup>2</sup> However, the further development of all-PSCs is severely limited by the lack of excellent polymer acceptors.<sup>3</sup> To date, only several specific polymer acceptors based on the naphthalene diimide (NDI) unit, perylenediimide (PDI) unit and B $\leftarrow$ N bridged thiophylthiazole (BNTT) unit can work as polymer acceptors for efficient all-PSCs with power conversion efficiencies (PCEs) exceeding 4%.<sup>4,5</sup>

<sup>a</sup>State Key Laboratory of Polymer Physics and Chemistry, Changchun Institute of Applied Chemistry, Chinese Academy of Sciences, Changchun 130022, People's Republic of China. E-mail: liujun@ciac.ac.cn; chuandong.dou@ciac.ac.cn

<sup>b</sup>University of Chinese Academy of Sciences, Beijing 100864, People's Republic of China

† Electronic supplementary information (ESI) available: Experimental details, thermal property, theoretical calculations, as well as all-PSC device fabrications and characterizations. See DOI: 10.1039/c6sc01756h

‡ Z. Ding and X. Long contributed equally to this work.

A key parameter for polymer acceptors is the lowest unoccupied molecular orbital (LUMO) energy level ( $E_{\text{LUMO}}$ ). In all-PSCs, the  $E_{\text{LUMO}}$  difference between the acceptor and donor ( $\Delta E_{\text{LUMO}}$ ) is regarded as the driving force for the charge separation.<sup>6</sup> The difference between the  $E_{\text{LUMO}}$  of the acceptor and the highest occupied molecular orbital (HOMO) energy level ( $E_{\text{HOMO}}$ ) of the donor is related to the open-circuit voltage ( $V_{\text{oc}}$ ) of all-PSCs.<sup>6</sup> Therefore, to get a large  $\Delta E_{\text{LUMO}}$  for effective charge separation and to maximize  $V_{\text{oc}}$ , the  $E_{\text{LUMO}}$  of the polymer acceptor must be carefully optimized. The state-of-the-art polymer acceptors are the NDI-based conjugated polymers.<sup>4</sup> Unfortunately, the  $E_{\text{LUMO}}$  of these polymers are fixed at *ca.* -3.85 eV and cannot be effectively tuned, leading to a low  $V_{\text{oc}}$  of the resulting all-PSCs. According to a study by Takimiya *et al.*,<sup>7</sup> the fixed  $E_{\text{LUMO}}$  of NDI-based polymers are due to the localized LUMOs on the NDI units. The  $E_{\text{LUMO}}$  of the NDI-based conjugated polymers are determined by the NDI unit and are not affected by the copolymerization units. Thus, it is important but challenging to develop polymer acceptors with tunable  $E_{\text{LUMO}}$ .

Following our strategy to develop polymer acceptors using the B $\leftarrow$ N unit,<sup>5</sup> we have reported a new electron-deficient building block based on the B $\leftarrow$ N unit, double B $\leftarrow$ N bridged bipyridine (BNBP), to develop a polymer acceptor.<sup>8</sup> In this manuscript, we report that BNBP-based polymer acceptors show tunable  $E_{\text{LUMO}}$  because of their delocalized LUMOs over the polymer backbones. The  $E_{\text{LUMO}}$  of the copolymer of the BNBP



unit and selenophene unit (**P-BNBP-Se**) is lower by 0.16 eV than that of the copolymer of the BNBP unit and thiophene unit (**P-BNBP-T**) (Fig. 1). As a result, the energy levels of **P-BNBP-Se** match well with the widely-used polymer donor, poly[(ethylhexyl-thiophenyl)-benzodithiophene-(ethylhexyl)-thienothiophene] (**PTB7-Th**).<sup>9</sup> While the all-PSC device based on the **PTB7-Th**:**P-BNBP-T** blend shows a moderate PCE of 2.27%, the corresponding device with **P-BNBP-Se** as the acceptor exhibits a PCE as high as 4.26% with a remarkably high  $V_{oc}$  of 1.03 V. These results indicate that BNBP-based polymer acceptors have different electronic structures from those of the classical NDI-based polymer acceptors and that they can give all-PSCs with remarkably high  $V_{oc}$  values and high PCEs.

## Results and discussion

Scheme 1 shows the synthetic route of **P-BNBP-Se** and **P-BNBP-T**. The three monomers were prepared following literature methods and the two polymers were synthesized in Stille-polymerization conditions.<sup>8</sup> Their chemical structures are confirmed by  $^1\text{H}$  NMR and elemental analysis. According to gel permeation chromatography (GPC), with 1,2,4-trichlorobenzene as the eluent at 150 °C, the number-average molecular weight ( $M_n$ ) and polydispersity (PDI) are 26.3 kDa and 1.93 for **P-BNBP-Se** and 46.2 kDa and 1.81 for **P-BNBP-T**, respectively. According to the thermogravimetric analysis (TGA), **P-BNBP-T** and **P-BNBP-Se** show a good thermal stability with thermal decomposition temperatures ( $T_d$ ) of over 350 °C (ESI†). In addition, the two polymers show a good solubility in common organic solvents, including chlorobenzene (CB), chloroform (CHCl<sub>3</sub>) and *o*-dichlorobenzene (*o*-DCB).

To elucidate the molecular orbitals of the two polymers, density functional theory (DFT) calculations at the B3LYP/6-31G\* level of theory were performed with the model compounds containing six repeating units with the long alkyl chains replaced by methyl groups.<sup>10</sup> For comparison, we also show the DFT calculation result of the state-of-the-art polymer acceptor, (poly(*N,N'*-bis(2-octyldecyl)-1,4,5,8-naphthalenedicarboximide-2,6-diyl)-alt-5,5'-(2,2-bithiophene))) (**N2200** or P(NDI2ODT2)) (Fig. 1a).<sup>11</sup> As shown in Fig. 2, the calculated LUMO of the model compound of **N2200** is localized on the NDI units, indicating that its  $E_{\text{LUMO}}$  is determined by the NDI unit and cannot be effectively tuned by changing the co-monomer units. This is consistent with the DFT calculation and experimental results of NDI-based conjugated polymers in the literature.<sup>4,11</sup> In contrast,

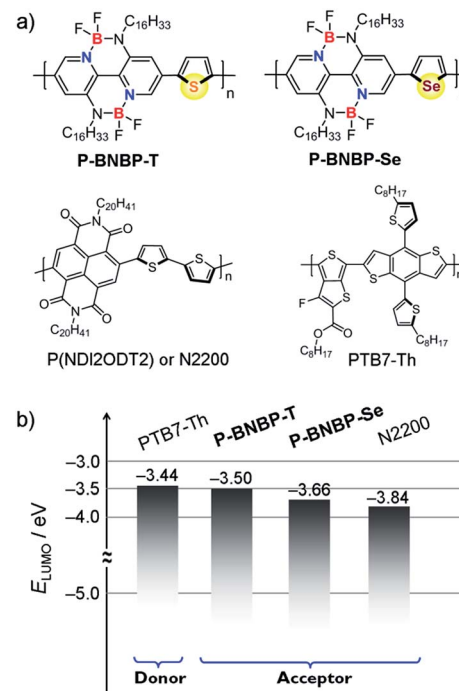
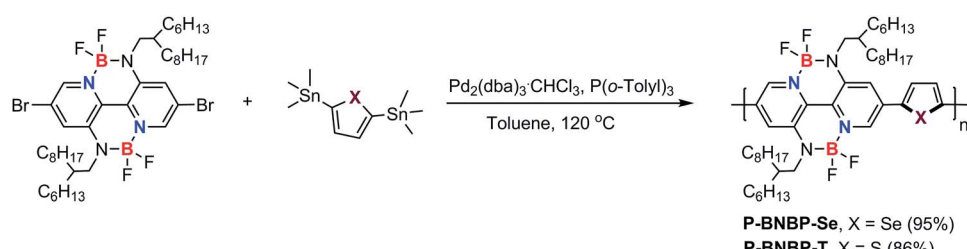


Fig. 1 (a) Chemical structures of **P-BNBP-Se**, **P-BNBP-T**, **N2200** and **PTB7-Th** and (b) their LUMO energy level alignments.

the calculated LUMOs of the model compounds of **P-BNBP-Se**/**P-BNBP-T** are delocalized over the BNBP units and the selenophene/thiophene units. Therefore, the LUMO levels of BNBP-based polymers are determined by both the BNBP unit and the co-monomer unit. The LUMO levels of BNBP-based polymers should be effectively tuned by changing the co-monomer units.

Cyclic voltammetry was employed to estimate the LUMO/HOMO energy levels of the two polymers (ESI†).<sup>12</sup> As shown in Fig. 3a, **P-BNBP-Se** exhibits irreversible reduction and oxidation waves with onset potentials of  $E_{\text{onset}}^{\text{red}} = -1.14$  V and  $E_{\text{onset}}^{\text{ox}} = +1.04$  V, respectively. Accordingly, the  $E_{\text{LUMO}}/\text{HOMO}$  of **P-BNBP-Se** are estimated to be  $-3.66$  eV/ $-5.84$  eV (Table 1). Similarly, the  $E_{\text{LUMO}}/\text{HOMO}$  of **P-BNBP-T** are estimated to be  $-3.50$  eV/ $-5.77$  eV (Table 1). As reported previously, the model compound of the BNBP unit itself has an  $E_{\text{LUMO}}$  of  $-3.19$  eV. The  $E_{\text{LUMO}}$  of the two BNBP-based polymers are much lower than that of the BNBP unit. Moreover, the  $E_{\text{LUMO}}$  of **P-BNBP-Se** is lower than that of **P-BNBP-T** by 0.16 eV. These results confirm that the LUMO levels of BNBP-based polymers can be effectively tuned by changing



Scheme 1 Synthetic route of **P-BNBP-Se** and **P-BNBP-T**.



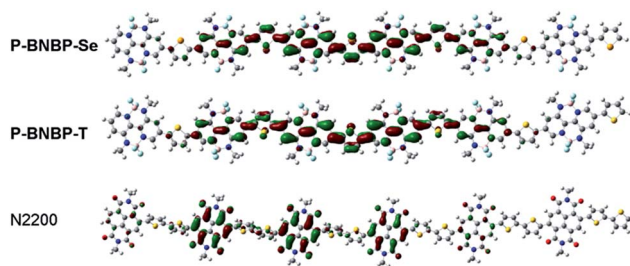


Fig. 2 Kohn–Sham LUMOs of model compounds of P-BNBP-Se, P-BNBP-T and N2200, based on calculations at the B3LYP/6–31G\* level.

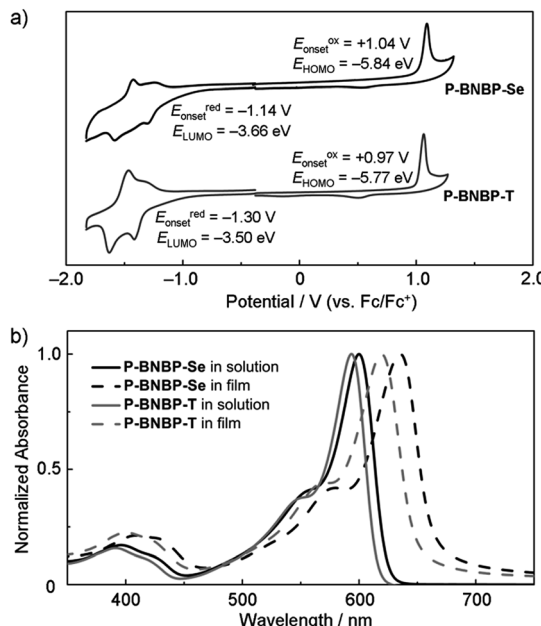


Fig. 3 (a) Cyclic voltammogram of P-BNBP-Se and P-BNBP-T in thin films using a Ag/AgCl reference electrode. Fc = ferrocene; (b) UV/Vis absorption spectra of P-BNBP-Se and P-BNBP-T in *o*-DCB solutions and in thin films.

the co-monomer units. This is consistent with the delocalized LUMOs in the DFT calculation results. The lower-lying  $E_{\text{LUMO}}$  of P-BNBP-Se is attributed to the lower electronegativity of the Se atom (2.4) than the S atom (2.5) and the empty orbital of the Se atom.<sup>13</sup>

Fig. 3b shows the absorption spectra of P-BNBP-Se and P-BNBP-T in dilute *o*-DCB solutions and in thin films. Both of the two polymers in solutions show broad absorption bands around

$\lambda = 580$  nm. The absorption spectrum is slightly redshifted for P-BNBP-Se compared to P-BNBP-T. In thin film, P-BNBP-Se exhibits a maximum absorption at 635 nm, while P-BNBP-T shows the absorption peak at 622 nm. Both of the two films show high absorption coefficients ( $\epsilon$ ), suggesting their intense light absorption. According to the onset absorption wavelength in thin films, the optical band gaps ( $E_g$ ) of P-BNBP-Se and P-BNBP-T are estimated to be 1.87 eV and 1.92 eV, respectively. The electron mobilities ( $\mu_e$ ) of P-BNBP-Se and P-BNBP-T were estimated using the space-charge-limited current (SCLC) method with the current density–voltage curves of the electron-only devices (device structure: ITO/PEIE/polymer/Ca/Al).<sup>14</sup> The electron mobility of P-BNBP-Se ( $\mu_e = 2.07 \times 10^{-4} \text{ cm}^2 \text{ V}^{-1} \text{ s}^{-1}$ ) is higher than that of P-BNBP-T ( $\mu_e = 7.16 \times 10^{-5} \text{ cm}^2 \text{ V}^{-1} \text{ s}^{-1}$ ) (ESI†). The higher electron mobility of P-BNBP-Se is due to the stronger intermolecular interactions in Se-containing polymers because of the larger and more polarizable radii of the selenium atom than the sulfur atom. This is confirmed by the smaller  $\pi$ – $\pi$  stacking distance of P-BNBP-Se ( $d_{\pi-\pi} = 3.77 \text{ \AA}$ ) than that of P-BNBP-T ( $d_{\pi-\pi} = 3.81 \text{ \AA}$ ) (ESI†). The electron mobility of P-BNBP-Se is comparable to the hole mobilities of typical polymer electron donors, which is very favourable for its application as a polymer electron acceptor in all-PSCs.

To investigate the application of P-BNBP-Se and P-BNBP-T as electron acceptors in all-PSCs, we select a widely-used polymer donor, PTB7-Th. All-PSC devices were fabricated with a configuration of ITO/PEDOT:PSS/PTB7-Th:P-BNBP-Se or P-BNBP-T/Ca/Al (ESI†). The active layer was spin-coated from the blend in *o*-DCB solution without any additives. Fig. 4 shows the current density–voltage ( $J$ – $V$ ) curves under AM 1.5G illumination (100 mW cm<sup>-2</sup>) and the external quantum efficiency (EQE) spectra of the optimal devices. The photovoltaic parameters are summarized in Table 2. The PTB7-Th : P-BNBP-T (3 : 1, w:w) device shows a PCE of 2.27% with a  $V_{\text{oc}}$  of 1.12 V, a short-circuit current density ( $J_{\text{sc}}$ ) of 5.24 mA cm<sup>-2</sup> and a fill factor (FF) of 0.39. The device based on the PTB7-Th : P-BNBP-Se (2 : 1, w:w) blend exhibits a PCE of 4.26% with a  $V_{\text{oc}}$  of 1.03 V, a  $J_{\text{sc}}$  of 10.02 mA cm<sup>-2</sup> and a FF of 0.42. This PCE value is comparable to that of the reference all-PSC device based on the PTB7-Th : N2200 (1 : 1, w:w) blend from the chloroform solution (PCE = 4.57%), indicating that P-BNBP-Se is an excellent polymer acceptor. Compared with the device of P-BNBP-T, the device of P-BNBP-Se shows a slightly decreased  $V_{\text{oc}}$  and much increased  $J_{\text{sc}}$ . The slightly decreased  $V_{\text{oc}}$  is attributed to the lower  $E_{\text{LUMO}}$  of P-BNBP-Se than that of P-BNBP-T. On the other hand, the  $V_{\text{oc}}$  of the P-BNBP-Se device is higher than that of the N2200 device by 0.22 V (Table 2) because the  $E_{\text{LUMO}}$  of P-BNBP-Se is higher than

Table 1 Molecular weights, photophysical and electronic properties, and electron mobilities of P-BNBP-Se and P-BNBP-T

Polymer	$M_n$ (kDa)	PDI	$\lambda_{\text{abs}}^a$ (nm)	$\lambda_{\text{abs}}^b$ (nm)	$\epsilon^b$ (cm <sup>-1</sup> )	$E_g^{\text{opt}b}$ (eV)	$E_{\text{onset}}^{\text{ox}}^c$ (V)	$E_{\text{onset}}^{\text{red}}^c$ (V)	$E_{\text{HOMO}}^d$ (eV)	$E_{\text{LUMO}}^d$ (eV)	$\mu_e$ (cm <sup>2</sup> V <sup>-1</sup> s <sup>-1</sup> )
P-BNBP-Se	26.3	1.93	600	635	$1.49 \times 10^5$	1.87	+1.04	-1.14	-5.84	-3.66	$2.07 \times 10^{-4}$
P-BNBP-T	46.0	2.01	593	622	$1.45 \times 10^5$	1.92	+0.97	-1.30	-5.77	-3.50	$7.16 \times 10^{-5}$

<sup>a</sup> Measured in *o*-DCB solution. <sup>b</sup> Measured in thin film. <sup>c</sup> Onset potential vs. Fc/Fc<sup>+</sup>. <sup>d</sup>  $E_{\text{HOMO/LUMO}} = -(4.80 + E_{\text{onset}}^{\text{ox}}/E_{\text{onset}}^{\text{red}})$  eV.



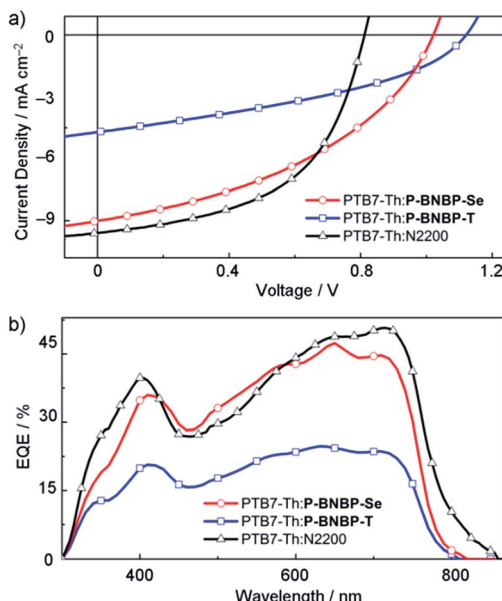


Fig. 4 (a)  $J$ – $V$  curves and (b) EQE spectra of the all-PSC devices based on the PTB7-Th:P-BNBP-Se, PTB7-Th:P-BNBP-T and PTB7-Th:N2200 blends, respectively.

Table 2 Summary of the all-PSC device performance

Acceptor	$V_{oc}$ (V)	$J_{sc}$ (mA cm <sup>-2</sup> )	FF	$PCE_{max/ave}^a$ (%)	EQE	$E_{loss}$ (eV)
P-BNBP-Se	1.03	10.02	0.42	4.26/4.11	0.47	0.56
P-BNBP-T	1.12	5.24	0.39	2.27/2.08	0.25	0.47
N2200	0.81	10.55	0.53	4.57/4.30	0.50	0.67

<sup>a</sup> The average PCE value is calculated from eight devices.

that of N2200. The much increased  $J_{sc}$  of the P-BNBP-Se device than that of the P-BNBP-T device is in accordance with their EQE values ( $EQE_{max} = 0.47$  for P-BNBP-Se and  $EQE_{max} = 0.25$  for P-BNBP-T) (Fig. 4b). The  $J_{sc}$  calculated from the integration of the EQE spectra agrees well with the  $J_{sc}$  values obtained from the  $J$ – $V$  scans within an error of 5%.

The charge carrier mobilities of the two blends were investigated using the SCLC method with the electron-only and hole-only devices (ESI†).<sup>14</sup> The electron mobility and hole mobility ( $\mu_h$ ) of the PTB7-Th:P-BNBP-Se blend are estimated to be  $3.34 \times 10^{-5}$  cm<sup>2</sup> V<sup>-1</sup> s<sup>-1</sup> and  $2.38 \times 10^{-4}$  cm<sup>2</sup> V<sup>-1</sup> s<sup>-1</sup>, respectively. In comparison, the PTB7-Th:P-BNBP-T blend exhibits a  $\mu_e = 5.96 \times 10^{-6}$  cm<sup>2</sup> V<sup>-1</sup> s<sup>-1</sup> and  $\mu_h = 7.28 \times 10^{-4}$  cm<sup>2</sup> V<sup>-1</sup> s<sup>-1</sup>, respectively. The higher electron mobility and the balanced electron/hole mobilities of the PTB7-Th:P-BNBP-Se blend are due to the enhanced electron mobility of P-BNBP-Se. We also investigated the bimolecular charge recombination in the all-PSC devices using the light-intensity dependence of the  $J$ – $V$  curves (Fig. 5). The  $J_{sc}$  follows a power-law dependence on the illumination intensity ( $J_{sc} \propto P_{light}^\alpha$ ), where  $P_{light}$  is light intensity and  $\alpha$  is the calculated power-law exponent. The  $\alpha$  values are 0.93 for the PTB7-Th:P-BNBP-Se device and 0.94 for the PTB7-

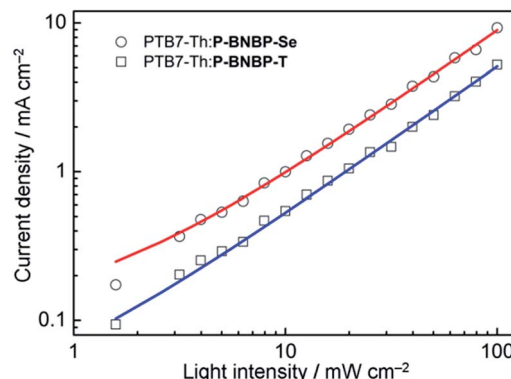


Fig. 5 Short-circuit current density ( $J_{sc}$ ) versus light intensity ( $P_{light}$ ) data and power-law ( $J_{sc} \propto P_{light}^\alpha$ ) fittings for the all-PSC devices.

Th:P-BNBP-T device, which are close to unity, suggesting that the bimolecular charge recombination is weak in the two devices at a short circuit condition.<sup>15</sup> Both the weak bimolecular recombination and the high and balanced electron/hole mobilities of PTB7-Th:P-BNBP-Se can explain its excellent device performance.

The morphologies of the PTB7-Th:P-BNBP-Se and PTB7-Th:P-BNBP-T blends were characterized by transmission electron microscopy (TEM) and atomic force microscopy (AFM). As shown in Fig. 6, the TEM images exhibit similar nano/micro-structures without large-size aggregation. The AFM images of the two blends similarly reveal smooth surface morphologies with the same root-mean-square (RMS) roughness of 1.47 nm and domain sizes of around 20–40 nm. The phase separation morphologies of the two blends are beneficial for good all-PSC devices.

In organic photovoltaics (OPVs), the  $\Delta E_{LUMO}$  of the donor and acceptor is regarded as the driving force for charge separation. The  $\Delta E_{LUMO}$  should be larger than a specific value for efficient charge separation. If  $\Delta E_{LUMO}$  is too large, there is a lot

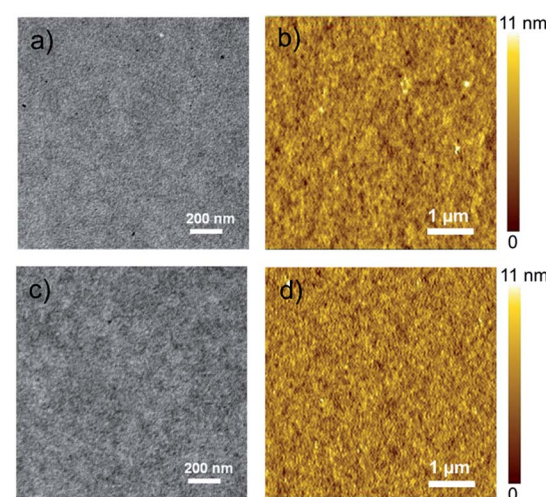


Fig. 6 The TEM images and the AFM height images of ((a) and (b)) the PTB7-Th:P-BNBP-Se blend and ((c) and (d)) the PTB7-Th:P-BNBP-T blend, respectively.

of energy loss in the charge separation process, leading to a low  $V_{oc}$  because the  $V_{oc}$  of OPVs is related to the difference between the  $E_{HOMO}$  of the donor and  $E_{LUMO}$  of the acceptor.<sup>6</sup> In our previous report, an all-PSC device based on the **PTB7:P-BNBP-T** blend ( $\Delta E_{LUMO} = 0.19$  eV) showed a good PCE of 3.38%.<sup>8</sup> As shown in Fig. 1b, the  $\Delta E_{LUMO}$  is only 0.06 eV for **PTB7-Th:P-BNBP-T**, and thus the all-PSC device shows a high  $V_{oc}$  but produces a low PCE due to the insufficient charge separation.<sup>4g</sup> As the  $E_{LUMO}$  of **P-BNBP-Se** is lower than that of **P-BNBP-T**, the  $\Delta E_{LUMO}$  for **PTB7-Th:P-BNBP-Se** is increased to 0.22 eV and ensures an efficient charge separation, resulting in higher  $J_{sc}$  and PCE values. Moreover, due to the suitable  $E_{LUMO}$  of **P-BNBP-Se**, the **PTB7-Th:P-BNBP-Se** device produces a high  $V_{oc}$  of 1.03 V, which is higher than that of the **PTB7-Th:N2200** device by 0.22 V. These results indicate that the suitable  $E_{LUMO}$  of **P-BNBP-Se** plays an important role in enhancing the all-PSCs device performance.

It is worthy to note the remarkably low photon energy losses ( $E_{loss}$ ) of the all-PSCs based on **P-BNBP-Se** and **P-BNBP-T**.  $E_{loss}$  is defined as the difference between the lowest optical bandgap of the donor/acceptor and the  $eV_{oc}$  of the organic photovoltaic (OPV) device ( $E_{loss} = E_g - eV_{oc}$ ).<sup>16</sup> Typically, OPVs have large  $E_{loss}$  values of 0.7–1.0 eV. It has been proposed that the lowest attainable  $E_{loss}$  of OPVs is 0.6 eV, despite several exceptional examples.<sup>17</sup> As listed in Table 2, the  $E_{loss}$  for the device of **PTB7-Th:P-BNBP-Se** and **PTB7-Th:P-BNBP-T** is 0.56 eV and 0.47 eV, respectively. To our best knowledge, the  $E_{loss}$  of 0.47 eV is the lowest one for OPVs reported so far. A small  $E_{loss}$  is always observed for all-PSCs with BNBP-based polymers as electron acceptors and the exact reason is as yet unknown. We speculate that the small  $E_{loss}$  is related to the high-lying LUMO levels of the BNBP-based polymers.

## Conclusions

In summary, we have developed a polymer acceptor based on the BNBP unit and selenophene unit with an optimal  $E_{LUMO}$  to simultaneously enable charge separation and maximize  $V_{oc}$ . BNBP-based polymers have delocalized LUMOs over the polymer backbones, so their  $E_{LUMO}$  can be tuned by changing the comonomer unit. The  $E_{LUMO}$  of **P-BNBP-Se** is lower by 0.16 eV than that of **P-BNBP-T** and consequently matches well with that of the polymer donor, **PTB7-Th**. While the all-PSC device based on **PTB7-Th:P-BNBP-T** shows a moderate PCE of 2.27%, the corresponding device with **P-BNBP-Se** as the acceptor exhibits a PCE as high as 4.26%. Moreover, the device of **P-BNBP-Se** shows a  $V_{oc}$  of up to 1.03 V and  $E_{loss}$  as small as 0.56 eV. These results indicate that BNBP-based polymer acceptors have different electronic structures from those of classical NDI-based polymer acceptors and that they can give all-PSCs with remarkably high  $V_{oc}$  values and high PCEs.

## Experimental section

### Synthesis of **P-BNBP-Se**

The dibromo-substituted BNBP monomer was synthesized according to the previous report.<sup>8</sup> The starting materials of the

dibromo-substituted BNBP monomer (220 mg, 0.248 mmol), 2,5-bis(trimethylstannyl)selenophene (114.1 mg, 0.248 mmol),  $Pd_2(dba)_3 \cdot CHCl_3$  (4.5 mg, 0.0050 mmol) and  $P(o\text{-tolyl})$  (12.1 mg, 0.04 mmol) were placed in a two-necked flask under argon, and then dried toluene (11 mL) was added. After the mixture was stirred at 115 °C for 48 h, an end-capping reaction was carried out by adding 2,5-bis(trimethylstannyl)selenophene (3 mg) and then bromobenzene (200 mg). After cooling, the resulting organic phase was extracted with  $CHCl_3$  (150 mL) and washed with water. After the solvents were removed, the residue was dispersed in methanol and the precipitate was collected. The obtained dark solid was dispersed in acetonitrile, and was collected and dried in a vacuum overnight. Yield: 213 mg (95%).  $^1H$  NMR (400 MHz,  $CDCl_3$ , 25 °C):  $\delta$  8.41 (s, 1H), 7.76 (s, 1H), 7.66 (s, 1H), 3.63 (br, 2H), 1.85 (br, 1H), 1.42–1.27 (br, 24H), 0.85 (br, 6H). GPC (TCB, polystyrene standard, 150 °C):  $M_n = 26\,300$ , PDI = 1.93. Anal. calcd for  $C_{46}H_{72}B_2F_4N_4Se$ : C, 64.42; H, 8.46; B, 2.52; F, 8.86; N, 6.53; Se, 9.21. Found: C, 64.25; H, 8.58; N, 6.65; Se, 9.05.

### Synthesis of **P-BNBP-T**

The starting materials of the dibromo-substituted BNBP monomer (150 mg, 0.166 mmol), 2,5-bis(trimethylstannyl)thiophene (68.5 mg, 0.166 mmol),  $Pd_2(dba)_3 \cdot CHCl_3$  (3.5 mg, 0.0033 mmol) and  $P(o\text{-tolyl})$  (8.1 mg, 0.027 mmol) were placed in a two-necked flask under argon, and then dried toluene (4 mL) was added. After the mixture was stirred at 115 °C for 50 h, an end-capping reaction was carried out by adding 2,5-bis(trimethylstannyl)thiophene (3 mg) and then bromobenzene (200 mg). After cooling, the resulting organic phase was extracted with  $CHCl_3$  (150 mL) and washed with water. After the solvents were removed, the residue was dispersed in methanol and the precipitate was collected. The obtained dark solid was dispersed in acetonitrile, and was collected and dried in a vacuum overnight. Yield: 116.5 mg (86%).  $^1H$  NMR (400 MHz,  $CDCl_3$ , 25 °C):  $\delta$  8.47 (s, 1H), 7.74 (s, 1H), 7.60 (s, 1H), 3.64 (br, 2H), 1.87 (br, 1H), 1.43–1.25 (br, 24H), 0.83 (br, 6H). GPC (TCB, polystyrene standard, 150 °C):  $M_n = 46\,200$ , PDI = 1.81. Anal. calcd for  $C_{46}H_{72}B_2F_4N_4S$ : C, 68.14; H, 8.95; B, 2.67; F, 7.37; N, 6.91; S, 3.95. Found: C, 67.83; H, 8.82; N, 6.75; S, 4.05.

## Acknowledgements

The authors are grateful for the financial support by the 973 Project (No. 2014CB643504), the Nature Science Foundation of China (No. 51373165, No. 21404099, No. 21574129), the “Thousand Talents Program” of China, the Strategic Priority Research Program of the Chinese Academy of Sciences (No. XDB12010200), and the State Key Laboratory of Supramolecular Structure and Materials in Jilin University (No. sklssm201608).

## Notes and references

- (a) T. Kim, J.-H. Kim, T. E. Kang, C. Lee, H. Kang, M. Shin, C. Wang, B. Ma, U. Jeong, T.-S. Kim and B. J. Kim, *Nat. Commun.*, 2015, **6**, 8547; (b) A. Facchetti, *Mater. Today*,



2013, **16**, 123; (c) G. Yu, J. Gao, J. C. Hummelen, F. Wudl and A. J. Heeger, *Science*, 1995, **270**, 1789.

2 (a) L. Gao, Z.-G. Zhang, L. Xue, J. Min, J. Zhang, Z. Wei and Y. Li, *Adv. Mater.*, 2016, **28**, 1884; (b) Y.-J. Hwang, B. A. E. Courtright, A. S. Ferreira, S. H. Tolbert and S. A. Jenekhe, *Adv. Mater.*, 2015, **27**, 4578; (c) Y.-J. Hwang, T. Earmme, B. A. E. Courtright, F. N. Eberle and S. A. Jenekhe, *J. Am. Chem. Soc.*, 2015, **137**, 4424; (d) T. Earmme, Y.-J. Hwang, S. Subramaniyan and S. A. Jenekhe, *Adv. Mater.*, 2014, **26**, 6080; (e) T. Earmme, Y.-J. Hwang, N. M. Murari, S. Subramaniyan and S. A. Jenekhe, *J. Am. Chem. Soc.*, 2013, **135**, 14960.

3 (a) H. Benten, D. Mori, H. Ohkita and S. Ito, *J. Mater. Chem. A*, 2016, **4**, 5340; (b) L. Lu, T. Zheng, Q. Wu, A. M. Schneider, D. Zhao and L. Yu, *Chem. Rev.*, 2015, **115**, 12666.

4 (a) N. Zhou, A. S. Dudnik, T. I. N. G. Li, E. F. Manley, T. J. Aldrich, P. Guo, H.-C. Liao, Z. Chen, L. X. Chen, R. P. H. Chang, A. Facchetti, M. O. de la Cruz and T. J. Marks, *J. Am. Chem. Soc.*, 2016, **138**, 1240; (b) C. Lee, H. Kang, W. Lee, T. Kim, K.-H. Kim, H. Y. Woo, C. Wang and B. J. Kim, *Adv. Mater.*, 2015, **27**, 2466; (c) H. Kang, M. A. Uddin, C. Lee, K.-H. Kim, T. L. Nguyen, W. Lee, Y. X. Li, C. Wang, H. Y. Woo and B. J. Kim, *J. Am. Chem. Soc.*, 2015, **137**, 2359; (d) J. W. Jung, J. W. Jo, C.-C. Chueh, F. Liu, W. H. Jo, T. P. Russell and A. K.-Y. Jen, *Adv. Mater.*, 2015, **27**, 3310; (e) L. Ye, X. Jiao, M. Zhou, S. Zhang, H. Yao, W. Zhao, A. Xia, H. Ade and J. Hou, *Adv. Mater.*, 2015, **27**, 6046; (f) P. Cheng, L. Ye, X. Zhao, J. Hou, Y. Li and X. Zhan, *Energy Environ. Sci.*, 2014, **7**, 1351; (g) Y. Zhou, T. Kurosawa, W. Ma, Y. Guo, L. Fang, K. Vandewal, Y. Diao, C. Wang, Q. Yan, J. Reinspach, J. Mei, A. L. Appleton, G. I. Koleilat, Y. Gao, S. C. B. Mannsfeld, A. Salleo, H. Ade, D. Zhao and Z. Bao, *Adv. Mater.*, 2014, **26**, 3767; (h) I. H. Jung, W.-Y. Lo, J. Jang, W. Chen, D. L. Zhao, E. S. Landry, L. Y. Lu, D. V. Talapin and L. Yu, *Chem. Mater.*, 2014, **26**, 3450; (i) C. Mu, P. Liu, W. Ma, K. Jiang, J. B. Zhao, K. Zhang, Z. H. Chen, Z. H. Wei, Y. Yi, J. N. Wang, S. H. Yang, F. Huang, A. Facchetti, H. Ade and H. Yan, *Adv. Mater.*, 2014, **26**, 7224; (j) D. Mori, H. Benten, I. Okada, H. Ohkita and S. Ito, *Energy Environ. Sci.*, 2014, **7**, 2939; (k) M. Schubert, B. A. Collins, H. Mangold, I. A. Howard, W. Schindler, K. Vandewal, S. Roland, J. Behrends, F. Krafft, R. Steyrleuthner, Z. Chen, K. Fostiroopoulos, R. Bittl, A. Salleo, A. Facchetti, F. Laquai, H. W. Ade and D. Neher, *Adv. Funct. Mater.*, 2014, **24**, 4068; (l) E. J. Zhou, J. Z. Cong, K. Hashimoto and K. Tajima, *Adv. Mater.*, 2013, **25**, 6991; (m) L. Xue, Y. Yang, Z.-G. Zhang, X. Dong, L. Gao, H. Bin, J. Zhang, Y. Yang and Y. Li, *J. Mater. Chem. A*, 2016, **4**, 5810.

5 (a) R. Zhao, C. Dou, Z. Xie, J. Liu and L. Wang, *Angew. Chem., Int. Ed.*, 2016, **55**, 5313; (b) C. Dou, Z. Ding, Z. Zhang, Z. Xie, J. Liu and L. Wang, *Angew. Chem., Int. Ed.*, 2015, **54**, 3648.

6 R. A. Street, *Adv. Mater.*, 2016, **28**, 3814.

7 K. Takimiya, I. Osaka and M. Nakano, *Chem. Mater.*, 2014, **26**, 587.

8 (a) C. Dou, X. Long, Z. Ding, Z. Xie, J. Liu and L. Wang, *Angew. Chem., Int. Ed.*, 2016, **55**, 1436; (b) X. Long, Z. Ding, C. Dou, J. Zhang, J. Liu and L. Wang, *Adv. Mater.*, 2016, DOI: 10.1002/adam.201601205.

9 Z. He, C. Zhong, S. Su, M. Xu, H. Wu and Y. Cao, *Nat. Photonics*, 2012, **6**, 591.

10 DFT calculations were performed using Gaussian 09 program: M. J. Frisch, *et al.*, *Gaussian 09, revision A.02*, Gaussian, Inc., Wallingford, CT, 2009. For details, see ESI.†

11 R. Steyrleuthner, M. Schubert, I. Howard, B. Klaumünzer, K. Schilling, Z. Chen, P. Saalfrank, F. Laquai, A. Facchetti and D. Neher, *J. Am. Chem. Soc.*, 2012, **134**, 18303.

12 Z. Ding, Z. Miao, Z. Xie and J. Liu, *J. Mater. Chem. A*, 2016, **4**, 2413.

13 (a) D. Meng, D. Sun, C. Zhong, T. Liu, B. Fan, L. Huo, Y. Li, W. Jiang, H. Choi, T. Kim, J. Y. Kim, Y. Sun, Z. Wang and A. J. Heeger, *J. Am. Chem. Soc.*, 2016, **138**, 375; (b) R. S. Ashraf, I. Meager, M. Nikolka, M. Kirkus, M. Planells, B. C. Schroeder, S. Holliday, M. Hurhangee, C. B. Nielsen, H. Sirringhaus and I. McCulloch, *J. Am. Chem. Soc.*, 2015, **137**, 1314.

14 P. W. M. Blom, M. J. M. de Jong and M. G. van Munster, *Phys. Rev. B: Solid State*, 1997, **55**, R656.

15 (a) A. K. K. Kywa, D. H. Wang, V. Gupta, W. L. Leong, L. Ke, G. C. Bazan and A. J. Heeger, *ACS Nano*, 2013, **7**, 4569; (b) S. R. Cowan, A. Roy and A. J. Heeger, *Phys. Rev. B: Condens. Matter Mater. Phys.*, 2010, **82**, 245207.

16 (a) R. A. J. Janssen and J. Nelson, *Adv. Mater.*, 2013, **25**, 1847; (b) D. Veldman, S. C. J. Meskers and R. A. J. Janssen, *Adv. Funct. Mater.*, 2009, **19**, 1939.

17 (a) K. Kawashima, Y. Tamai, H. Ohkita, I. Osaka and K. Takimiya, *Nat. Commun.*, 2015, **6**, 10085; (b) W. Li, K. H. Hendriks, A. Furlan, M. M. Wienk and R. A. J. Janssen, *J. Am. Chem. Soc.*, 2015, **137**, 2231; (c) M. Wang, H. Wang, T. Yokoyama, X. Liu, Y. Huang, Y. Zhang, T.-Q. Nguyen, S. Aramaki and G. C. Bazan, *J. Am. Chem. Soc.*, 2014, **136**, 12576.

